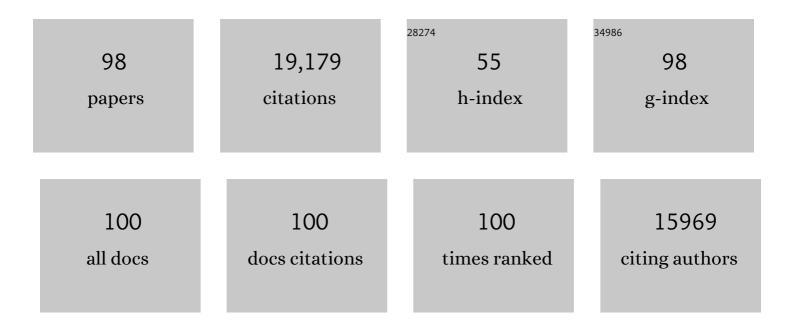
Tao Yao

List of Publications by Year in descending order

Source: https://exaly.com/author-pdf/1772796/publications.pdf Version: 2024-02-01



ΤΛΟΥΛΟ

#	Article	IF	CITATIONS
1	Laser-assisted high-performance PtRu alloy for pH-universal hydrogen evolution. Energy and Environmental Science, 2022, 15, 102-108.	30.8	66
2	Synergistic Modulation at Atomically Dispersed Fe/Au Interface for Selective CO ₂ Electroreduction. Nano Letters, 2021, 21, 686-692.	9.1	41
3	Single Atomic Cerium Sites with a High Coordination Number for Efficient Oxygen Reduction in Proton-Exchange Membrane Fuel Cells. ACS Catalysis, 2021, 11, 3923-3929.	11.2	156
4	In Situ Investigation on Doping Effect in Co-Doped Tungsten Diselenide Nanosheets for Hydrogen Evolution Reaction. Journal of Physical Chemistry C, 2021, 125, 6229-6236.	3.1	16
5	Dualâ€Metal Sites Boosting Polarization of Nitrogen Molecules for Efficient Nitrogen Photofixation. Advanced Science, 2021, 8, 2100302.	11.2	32
6	Synergistically electronic tuning of metalloid CdSe nanorods for enhanced electrochemical CO2 reduction. Science China Materials, 2021, 64, 2997-3006.	6.3	20
7	Relationship between Voltage Hysteresis and Voltage Decay in Lithium-Rich Layered Oxide Cathodes. Journal of Physical Chemistry C, 2021, 125, 16913-16920.	3.1	12
8	Atomically Precise Dinuclear Site Active toward Electrocatalytic CO ₂ Reduction. Journal of the American Chemical Society, 2021, 143, 11317-11324.	13.7	153
9	Regulating the Coordination Environment of Ruthenium Cluster Catalysts for the Alkaline Hydrogen Evolution Reaction. Journal of Physical Chemistry Letters, 2021, 12, 8016-8023.	4.6	21
10	Surface Oxygen Injection in Tin Disulfide Nanosheets for Efficient CO2 Electroreduction to Formate and Syngas. Nano-Micro Letters, 2021, 13, 189.	27.0	36
11	Insight into Fe Activating One-Dimensional α-Ni(OH) ₂ Nanobelts for Efficient Oxygen Evolution Reaction. Journal of Physical Chemistry C, 2021, 125, 20301-20308.	3.1	17
12	Plasmon-assisted photocatalytic CO ₂ reduction on Au decorated ZrO ₂ catalysts. Dalton Transactions, 2021, 50, 6076-6082.	3.3	16
13	Simultaneous oxidative and reductive reactions in one system by atomic design. Nature Catalysis, 2021, 4, 134-143.	34.4	132
14	A reasonable approach for the generation of hollow icosahedral kernels in metal nanoclusters. Nature Communications, 2021, 12, 6186.	12.8	12
15	Substrate strain tunes operando geometric distortion and oxygen reduction activity of CuN2C2 single-atom sites. Nature Communications, 2021, 12, 6335.	12.8	95
16	XAFS study on single-atomic-site Cu1/N-graphene catalyst for oxygen reduction reaction. Radiation Physics and Chemistry, 2020, 175, 108230.	2.8	11
17	Dynamic Surface Reconstruction of Single-Atom Bimetallic Alloy under <i>Operando</i> Electrochemical Conditions. Nano Letters, 2020, 20, 8319-8325.	9.1	28
18	Active Sites of Single-Atom Iron Catalyst for Electrochemical Hydrogen Evolution. Journal of Physical Chemistry Letters, 2020, 11, 6691-6696.	4.6	37

#	Article	IF	CITATIONS
19	Atomic Filtration by Graphene Oxide Membranes to Access Atomically Dispersed Single Atom Catalysts. ACS Catalysis, 2020, 10, 10468-10475.	11.2	36
20	Dehydrogenation of Ethylene on Supported Palladium Nanoparticles: A Double View from Metal and Hydrocarbon Sides. Nanomaterials, 2020, 10, 1643.	4.1	14
21	<i>Operando</i> evidence of Cu ⁺ stabilization <i>via</i> a single-atom modifier for CO ₂ electroreduction. Journal of Materials Chemistry A, 2020, 8, 25970-25977.	10.3	26
22	Iridium single-atom catalyst on nitrogen-doped carbon for formic acid oxidation synthesized using a general host–guest strategy. Nature Chemistry, 2020, 12, 764-772.	13.6	452
23	Single Iron Site Nanozyme for Ultrasensitive Glucose Detection. Small, 2020, 16, e2002343.	10.0	103
24	Cation-Exchange Induced Precise Regulation of Single Copper Site Triggers Room-Temperature Oxidation of Benzene. Journal of the American Chemical Society, 2020, 142, 12643-12650.	13.7	110
25	N-Coordinated Dual-Metal Single-Site Catalyst for Low-Temperature CO Oxidation. ACS Catalysis, 2020, 10, 2754-2761.	11.2	112
26	Uncovering near-free platinum single-atom dynamics during electrochemical hydrogen evolution reaction. Nature Communications, 2020, 11, 1029.	12.8	379
27	Strong Ni–S Hybridization in a Crystalline NiS Electrocatalyst for Robust Acidic Oxygen Evolution. Journal of Physical Chemistry C, 2020, 124, 2756-2761.	3.1	20
28	Recover the activity of sintered supported catalysts by nitrogen-doped carbon atomization. Nature Communications, 2020, 11, 335.	12.8	69
29	Coordination-Engineered Cu–N _{<i>x</i>} Single-Site Catalyst for Enhancing Oxygen Reduction Reaction. ACS Applied Energy Materials, 2019, 2, 6497-6504.	5.1	58
30	Dynamic oxygen adsorption on single-atomic Ruthenium catalyst with high performance for acidic oxygen evolution reaction. Nature Communications, 2019, 10, 4849.	12.8	416
31	A Supported Nickel Catalyst Stabilized by a Surface Digging Effect for Efficient Methane Oxidation. Angewandte Chemie, 2019, 131, 18559-18564.	2.0	20
32	A Supported Nickel Catalyst Stabilized by a Surface Digging Effect for Efficient Methane Oxidation. Angewandte Chemie - International Edition, 2019, 58, 18388-18393.	13.8	69
33	Atomically dispersed iron hydroxide anchored on Pt for preferential oxidation of CO in H2. Nature, 2019, 565, 631-635.	27.8	423
34	Unraveling the enzyme-like activity of heterogeneous single atom catalyst. Chemical Communications, 2019, 55, 2285-2288.	4.1	205
35	Unconventional CN vacancies suppress iron-leaching in Prussian blue analogue pre-catalyst for boosted oxygen evolution catalysis. Nature Communications, 2019, 10, 2799.	12.8	202
36	Engineering the electronic structure of single atom Ru sites via compressive strain boosts acidic water oxidation electrocatalysis. Nature Catalysis, 2019, 2, 304-313.	34.4	757

#	Article	IF	CITATIONS
37	Efficient and Robust Carbon Dioxide Electroreduction Enabled by Atomically Dispersed Sn <i>^{l´}</i> ⁺ Sites. Advanced Materials, 2019, 31, e1808135.	21.0	321
38	Engineering the Electronic Structure of Submonolayer Pt on Intermetallic Pd ₃ Pb via Charge Transfer Boosts the Hydrogen Evolution Reaction. Journal of the American Chemical Society, 2019, 141, 19964-19968.	13.7	99
39	Regulating the coordination environment of Co single atoms for achieving efficient electrocatalytic activity in CO2 reduction. Applied Catalysis B: Environmental, 2019, 240, 234-240.	20.2	224
40	Identification of single-atom active sites in carbon-based cobalt catalysts during electrocatalytic hydrogen evolution. Nature Catalysis, 2019, 2, 134-141.	34.4	629
41	Regulation of Coordination Number over Single Co Sites: Triggering the Efficient Electroreduction of CO ₂ . Angewandte Chemie - International Edition, 2018, 57, 1944-1948.	13.8	888
42	Regulation of Coordination Number over Single Co Sites: Triggering the Efficient Electroreduction of CO ₂ . Angewandte Chemie, 2018, 130, 1962-1966.	2.0	244
43	A single palladium site catalyst as a bridge for converting homogeneous to heterogeneous in dimerization of terminal aryl acetylenes. Materials Chemistry Frontiers, 2018, 2, 1317-1322.	5.9	23
44	Grain boundaries modulating active sites in RhCo porous nanospheres for efficient CO2 hydrogenation. Nano Research, 2018, 11, 2357-2365.	10.4	21
45	Synergistic effect of well-defined dual sites boosting the oxygen reduction reaction. Energy and Environmental Science, 2018, 11, 3375-3379.	30.8	528
46	Single Pt Atom with Highly Vacant d-Orbital for Accelerating Photocatalytic H ₂ Evolution. ACS Applied Energy Materials, 2018, 1, 6082-6088.	5.1	93
47	Coupling confinement activating cobalt oxide ultra-small clusters for high-turnover oxygen evolution electrocatalysis. Journal of Materials Chemistry A, 2018, 6, 15684-15689.	10.3	25
48	Efficient and Robust Hydrogen Evolution: Phosphorus Nitride Imide Nanotubes as Supports for Anchoring Single Ruthenium Sites. Angewandte Chemie - International Edition, 2018, 57, 9495-9500.	13.8	205
49	Atomic layer confined vacancies for atomic-level insights into carbon dioxide electroreduction. Nature Communications, 2017, 8, 14503.	12.8	365
50	Carbon Dioxide Electroreduction into Syngas Boosted by a Partially Delocalized Charge in Molybdenum Sulfide Selenide Alloy Monolayers. Angewandte Chemie, 2017, 129, 9249-9253.	2.0	154
51	Integration of plasmonic and amorphous effects in MoO _{3â^'x} spheres for efficient photoelectrochemical water oxidation. Journal of Materials Chemistry A, 2017, 5, 12022-12026.	10.3	28
52	lonic Exchange of Metal–Organic Frameworks to Access Single Nickel Sites for Efficient Electroreduction of CO ₂ . Journal of the American Chemical Society, 2017, 139, 8078-8081.	13.7	1,115
53	Single‣ite Active Cobaltâ€Based Photocatalyst with a Long Carrier Lifetime for Spontaneous Overall Water Splitting. Angewandte Chemie - International Edition, 2017, 56, 9312-9317.	13.8	393
54	Single‧ite Active Cobaltâ€Based Photocatalyst with a Long Carrier Lifetime for Spontaneous Overall Water Splitting. Angewandte Chemie, 2017, 129, 9440-9445.	2.0	95

#	Article	IF	CITATIONS
55	Carbon Dioxide Electroreduction into Syngas Boosted by a Partially Delocalized Charge in Molybdenum Sulfide Selenide Alloy Monolayers. Angewandte Chemie - International Edition, 2017, 56, 9121-9125.	13.8	205
56	Single Ni sites distributed on N-doped carbon for selective hydrogenation of acetylene. Chemical Communications, 2017, 53, 11568-11571.	4.1	88
57	Bottom-up precise synthesis of stable platinum dimers on graphene. Nature Communications, 2017, 8, 1070.	12.8	466
58	Frontispiece: Singleâ€&ite Active Cobaltâ€Based Photocatalyst with a Long Carrier Lifetime for Spontaneous Overall Water Splitting. Angewandte Chemie - International Edition, 2017, 56, .	13.8	1
59	Strong Surface Hydrophilicity in Co-Based Electrocatalysts for Water Oxidation. ACS Applied Materials & Interfaces, 2017, 9, 26867-26873.	8.0	57
60	Frontispiz: Singleâ€Site Active Cobaltâ€Based Photocatalyst with a Long Carrier Lifetime for Spontaneous Overall Water Splitting. Angewandte Chemie, 2017, 129, .	2.0	0
61	Atomic‣evel Insight into Optimizing the Hydrogen Evolution Pathway over a Co ₁ â€N ₄ Single‧ite Photocatalyst. Angewandte Chemie, 2017, 129, 12359-12364.	2.0	36
62	Atomic‣evel Insight into Optimizing the Hydrogen Evolution Pathway over a Co ₁ â€N ₄ Single‣ite Photocatalyst. Angewandte Chemie - International Edition, 2017, 56, 12191-12196.	13.8	269
63	Design of N-Coordinated Dual-Metal Sites: A Stable and Active Pt-Free Catalyst for Acidic Oxygen Reduction Reaction. Journal of the American Chemical Society, 2017, 139, 17281-17284.	13.7	1,220
64	Synergetic enhancement of plasmonic hot-electron injection in Au cluster-nanoparticle/C ₃ N ₄ for photocatalytic hydrogen evolution. Journal of Materials Chemistry A, 2017, 5, 19649-19655.	10.3	61
65	High-Content Metallic 1T Phase in MoS ₂ -Based Electrocatalyst for Efficient Hydrogen Evolution. Journal of Physical Chemistry C, 2017, 121, 15071-15077.	3.1	85
66	Uncoordinated Amine Groups of Metal–Organic Frameworks to Anchor Single Ru Sites as Chemoselective Catalysts toward the Hydrogenation of Quinoline. Journal of the American Chemical Society, 2017, 139, 9419-9422.	13.7	558
67	Oxyhydroxide Nanosheets with Highly Efficient Electron–Hole Pair Separation for Hydrogen Evolution. Angewandte Chemie, 2016, 128, 2177-2181.	2.0	26
68	Oxyhydroxide Nanosheets with Highly Efficient Electron–Hole Pair Separation for Hydrogen Evolution. Angewandte Chemie - International Edition, 2016, 55, 2137-2141.	13.8	99
69	Enhanced Photoexcited Carrier Separation in Oxygenâ€Doped ZnIn ₂ S ₄ Nanosheets for Hydrogen Evolution. Angewandte Chemie - International Edition, 2016, 55, 6716-6720.	13.8	454
70	Partial-surface-passivation strategy for transition-metal-based copper–gold nanocage. Chemical Communications, 2016, 52, 6617-6620.	4.1	12
71	Single Cobalt Atoms with Precise Nâ€Coordination as Superior Oxygen Reduction Reaction Catalysts. Angewandte Chemie - International Edition, 2016, 55, 10800-10805.	13.8	1,836
72	Single Cobalt Atoms with Precise Nâ€Coordination as Superior Oxygen Reduction Reaction Catalysts. Angewandte Chemie, 2016, 128, 10958-10963.	2.0	373

#	Article	IF	CITATIONS
73	Enhanced Photoexcited Carrier Separation in Oxygenâ€Doped ZnIn ₂ S ₄ Nanosheets for Hydrogen Evolution. Angewandte Chemie, 2016, 128, 6828-6832.	2.0	42
74	Solvent-induced desorption of alkanethiol ligands from Au nanoparticles. Physical Chemistry Chemical Physics, 2016, 18, 15927-15933.	2.8	6
75	CoOOH Nanosheets with High Mass Activity for Water Oxidation. Angewandte Chemie - International Edition, 2015, 54, 8722-8727.	13.8	547
76	Ultrathin CoOOH Oxides Nanosheets Realizing Efficient Photocatalytic Hydrogen Evolution. Journal of Physical Chemistry C, 2015, 119, 26362-26366.	3.1	43
77	Vacancy-Induced Ferromagnetism of MoS ₂ Nanosheets. Journal of the American Chemical Society, 2015, 137, 2622-2627.	13.7	659
78	X-ray absorption fine structure spectroscopy in nanomaterials. Science China Materials, 2015, 58, 313-341.	6.3	112
79	Single-Atom Pd ₁ /Graphene Catalyst Achieved by Atomic Layer Deposition: Remarkable Performance in Selective Hydrogenation of 1,3-Butadiene. Journal of the American Chemical Society, 2015, 137, 10484-10487.	13.7	905
80	Realizing Ferromagnetic Coupling in Diluted Magnetic Semiconductor Quantum Dots. Journal of the American Chemical Society, 2014, 136, 1150-1155.	13.7	27
81	Graphene Activating Room-Temperature Ferromagnetic Exchange in Cobalt-Doped ZnO Dilute Magnetic Semiconductor Quantum Dots. ACS Nano, 2014, 8, 10589-10596.	14.6	44
82	Aligned Fe2TiO5-containing nanotube arrays with low onset potential for visible-light water oxidation. Nature Communications, 2014, 5, 5122.	12.8	161
83	ZnO@S-doped ZnO core/shell nanocomposites for highly efficient solar water splitting. Journal of Power Sources, 2014, 269, 24-30.	7.8	22
84	Solvent Influence on the Role of Thiols in Growth of Thiols-Capped Au Nanocrystals. Journal of Physical Chemistry C, 2014, 118, 714-719.	3.1	25
85	Unidirectional Thermal Diffusion in Bimetallic Cu@Au Nanoparticles. ACS Nano, 2014, 8, 1886-1892.	14.6	48
86	Ultrathin Nanosheets of Halfâ€Metallic Monoclinic Vanadium Dioxide with a Thermally Induced Phase Transition. Angewandte Chemie - International Edition, 2013, 52, 7554-7558.	13.8	52
87	XAFS in dilute magnetic semiconductors. Dalton Transactions, 2013, 42, 13779.	3.3	42
88	Adsorption kinetic process of thiol ligands on gold nanocrystals. Nanoscale, 2013, 5, 11795.	5.6	23
89	Modifying the Atomic and Electronic Structures of Gold Nanocrystals via Changing the Chain Length of <i>n</i> -Alkanethiol Ligands. Journal of Physical Chemistry C, 2012, 116, 24999-25003.	3.1	16
90	Controllable synthesis of gold nanoparticles with ultrasmall size and high monodispersity via continuous supplement of precursor. Dalton Transactions, 2012, 41, 11725.	3.3	27

#	Article	IF	CITATIONS
91	Probing Nucleation Pathways for Morphological Manipulation of Platinum Nanocrystals. Journal of the American Chemical Society, 2012, 134, 9410-9416.	13.7	71
92	Ni-Doped Overlayer Hematite Nanotube: A Highly Photoactive Architecture for Utilization of Visible Light. Journal of Physical Chemistry C, 2012, 116, 24060-24067.	3.1	69
93	Hexane-Driven Icosahedral to Cuboctahedral Structure Transformation of Gold Nanoclusters. Journal of the American Chemical Society, 2012, 134, 17997-18003.	13.7	70
94	Mediating distribution of magnetic Co ions by Cr-codoping in (Co,Cr): ZnO thin films. Applied Physics Letters, 2010, 97, 042504.	3.3	15
95	Determination of the role of O vacancy in Co:ZnO magnetic film. Journal of Applied Physics, 2010, 108, .	2.5	20
96	Understanding the Nature of the Kinetic Process in a <mml:math xmlns:mml="http://www.w3.org/1998/Math/MathML" display="inline"><mml:msub><mml:mi>VO</mml:mi><mml:mn>2</mml:mn></mml:msub>Metal-In: Transition. Physical Review Letters, 2010, 105, 226405.</mml:math 	sulator	171
97	Insights into Initial Kinetic Nucleation of Gold Nanocrystals. Journal of the American Chemical Society, 2010, 132, 7696-7701.	13.7	151
98	High-Temperature Ferromagnetism of Hybrid Nanostructure Agâ´'Zn0.92Co0.08O Dilute Magnetic Semiconductor. Journal of Physical Chemistry C, 2009, 113, 3581-3585.	3.1	17